Instrumentation

Upgrading A Scintillation Camera—A Comparative Study

Herbert Strauss, Donald Faulkner*, Marlene Garone*, Margaret Roman*, James Giel, Mary Jane Zarzycki, and Eva Nikawitz

Veterans Administration Medical Center, East Orange, New Jersey

We upgraded a scintillation camera from a 19PM-tube Pho/Gamma HP to a 37-tube unit Pho/Gamma 37 GP. A variety of commercially available phantoms was carefully imaged before and after upgrading. In order to assure study credibility, the same collimators, photographic systems, window widths, and baseline values were used throughout. Source activities were maintained as closely as possible. All comparative studies were preset to the same number of counts, and the other parameters used to assure study credibility were kept constant. Greatly increased spatial resolution of the upgraded system and consequent improved lesion detectability are demonstrated.

Modern scintillation cameras have 37 or more photomultiplier (PM) tubes compared to 19 tubes on older cameras. The increased number of PM tubes has contributed to improving the overall performance of cameras (*1*). The need for improved performance has become increasingly important with the advent of newer procedures such as myocardial imaging with thallium-201. One economical way to obtain a 37PM-tube camera is to upgrade an existing camera already in the field and several manufacturers have this capability. We compared the Searle Pho/Gamma HP, a 19PM-tube camera (phase 1), to the Pho/Gamma 37 GP (Searle Radiographics, Inc., Des Plaines, IL), after its conversion to a 37-tube unit (phase 2).

Certain technical modifications involved in the camera upgrading are pertinent to this evaluation. In the detector head, the number of PM tubes was increased from 19 to 37 and a new crystal was installed. New preamplifier assemblies associated with each PM tube were installed, which incorporated revision and preintegration for increased resolution. In the analyzer module of the camera console, a new isotope range switch and seven updated printed circuit boards were installed for compatibility with the new detector head. Other changes included a new L.E.D. scaler and high stability power supply unit.

All remaining components were not changed during this upgrading and are responsible for the validity of this comparison. The same collimators were used with both cameras. The photographic equipment used with each camera was the same, including triple and single lens Polaroid units and a micro dot imager interfaced with a Data-Store/Playback system (supplied by Searle). In addition, each camera was tuned for optimum performance by the same manufacturer's service engineer.

Comparison of the cameras was based mainly on a study of two performance parameters: plane sensitivity and spatial resolution. According to Rollo (*2*), "Plane sensitivity is the counts per second recorded by the imaging device for each disintegration per second per square centimeter occuring within a plane sheet of radioactivity. Spatial resolution may be defined as the fidelity with which the imaging device reproduces the activity distribution of an object in the image plane."

Materials, Methods, and Results

In order to determine spatial resolution, a variety of commercially available phantoms was carefully imaged before and after upgrading. Source activities were kept as similar as possible, and gamma energies, window widths, and baseline settings were identical in both parts of the study. Point sources were obtained by placing the designated number of millicuries in a lead pig with a tiny aperature drilled in the top. All comparative studies were preset to the same number of counts and other parameters, such as collimators and photographic systems, were kept constant to assure credibility.

In addition, an anatomical phantom supplied by the College of American Pathologists was imaged. This phantom simulates a clinical situation. We used a Rollo phantom in an attempt to quantitate the imaging ability of each camera and a flood source was used to measure the plane sensitivity.

Plane sensitivity was evaluated for each camera using a 10 × 10 in. Tc-99m-filled flood source. Counts were accumulated with the flood source at the surface of the

For reprints contact: Herbert D. Strauss, Nuclear Medicine Service, V.A. Medical Center, East Orange, NJ 07019.

*Student, John F. Kennedy Medical Center School of Nuclear Medicine Technology, Edison, NJ.

high resolution collimator. The mean value of counts per minute (cpm) was determined and a value for cpm/μCi/cm^2 was calculated. The 19PM-tube camera recorded a Tc-99m activity of 1.55 mCi for a mean value of 307,170 cpm or 0.39 cpm/μCi/cm^2. The 37PM-tube camera recorded a Tc-99m activity of 1.85 mCi for a mean value of 310,245 cpm or 0.33 cpm/μCi/cm^2.

Several commercially available imaging phantoms were utilized in order to compare spatial resolution. A four quadrant bar phantom was used to determine intrinsic resolution. A point source of Tc-99m of 160 mCi was used in phase 1, and 127 mCi in phase 2. Two million counts were obtained per image; results are shown in Fig. 1. The 19PM-tube camera resolved only the 4.5-mm quadrant, whereas the 37PM-tube camera effectively resolved the 4.5-, 4.0-, 3.5-, and 3.0-mm quadrants.

A different four quadrant bar phantom was utilized to evaluate resolution at increasing distances from the detector. Using the high sensitivity collimator, a Tc-99m filled flood source with activities of 4.0 mCi, phase 1 and 4.5 mCi, phase 2, was imaged for 2 million counts at 1 in. depth intervals. No attenuating medium was used between the phantom and the detector. The 19PM-tube camera lost ability to resolve the $^3/_{16}$ in. quadrant at 1 in. distance; whereas the 37-tube camera maintained resolution of all quadrants out to 2 in. from the detector (Fig. 2).

The Hine-Duley phantom was utilized to evaluate intrinsic resolution by determining the smallest resolvable bar thickness. This phantom was imaged using Tc-99m point sources of 120 mCi, phase 1 and 150 mCi, phase 2. Two million counts were obtained per image. The 19PM-tube camera could not resolve the $^5/_{32}$ in. section. The 37PM-tube camera resolved the $^5/_{32}$ and $^3/_{16}$ in. bar clearly (Fig. 3).

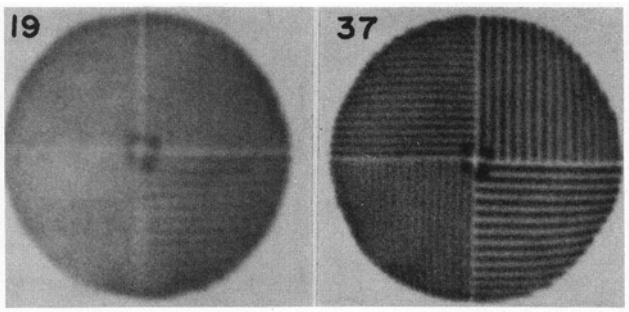

FIG. 1. Four quadrant bar phantom shows intrinsic resolution. Note ability to resolve 3-mm bar with 37 GP as compared to 4.5 mm with HP camera.

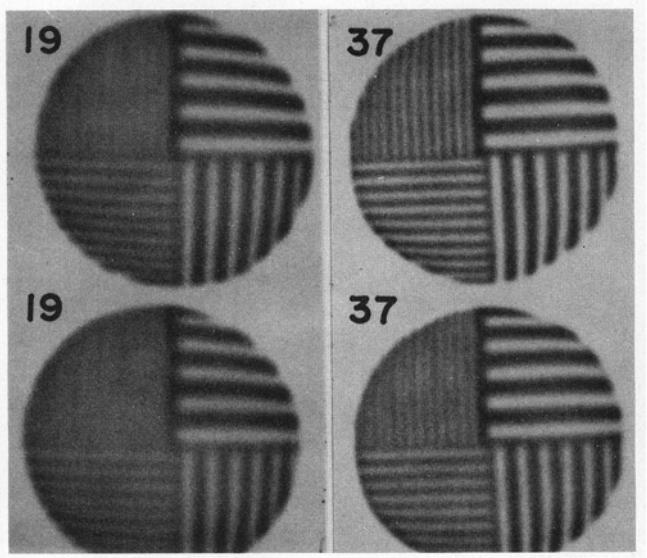

FIG. 2. Four quadrant bar phantom compared for depth resolution using high sensitivity collimator. Note that at surface of collimator, all bars are resolvable for both cameras; however, at 1 in. depth, 3/16 in. bars are no longer resolved with HP camera.

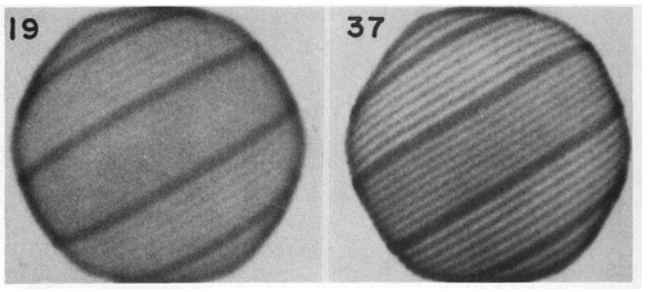

FIG. 3. Hine-Duley bar phantom intrinsic resolution: note ability to image 5/32 in. bars with 37 GP, as compared to 3/16 in. bars with HP camera.

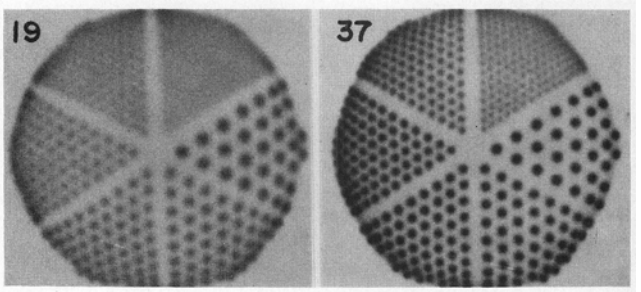

FIG. 4. Anger high resolution phantom shows intrinsic resolution. Note ability to resolve 2-mm holes with 37 GP, as compared to 3 mm with HP camera.

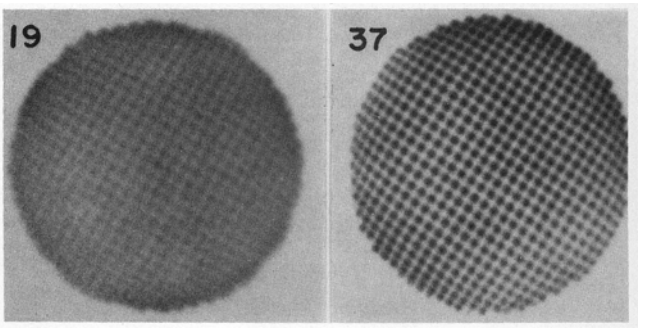

FIG. 5. Smith orthogonal hole phantom shows intrinsic resolution. Note ability to better resolve 3/16 in. hole diameter with 37 GP camera.

The Anger high resolution phantom was utilized to evaluate intrinsic resolution by determining the smallest resolvable hole diameter. The phantom was imaged using Tc-99m point sources of 120 mCi, phase 1 and 150 mCi, phase 2. Two million counts were obtained per image. The 19PM-tube camera resolved down to the third largest, the 3-mm diameter holes. The 37PM-tube camera resolved all holes including the smallest, the 2-mm size (Fig. 4).

The Smith orthogonal hole phantom (SOH) was used to evaluate intrinsic resolution. The $^3/_{16}$ in. hole diameter SOH phantom was imaged using Tc-99m point sources of 105 mCi, phase 1 and 91 mCi, phase 2. Two million counts were obtained per image. The 19PM-tube camera poorly resolved the $^3/_{16}$ in. holes, whereas the 37PM-tube camera clearly resolved them (Fig. 5).

The CAP 1975 series X-B phantom simulates the skeletal structure of the anterior and posterior chest. Lesions are simulated by Co-57 activity in a ratio of 1.25:1 compared to simulated normal bone activity. Activity was located at $1^1/_2$ in. below the phantom surface in the posterior view. Figures 6 and 7 depict the size and location of each lesion within the phantom. The 19PM-tube camera was unable to resolve lesions 3H (1.0-cm diameter) and 8H (0.8 cm) anteriorly, and lesions 3H (1.2 cm) posteriorly. The 37PM-tube camera resolved all lesions in both views, (Figs. 8 and 9). Then 500,000 counts were obtained per image using the high sensitivity collimator.

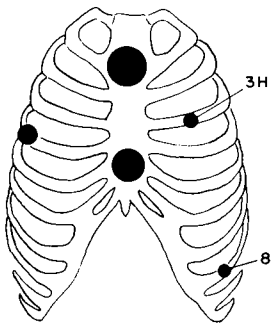

FIG. 6. CAP phantom, anterior aspect, shows size and position of to be imaged.

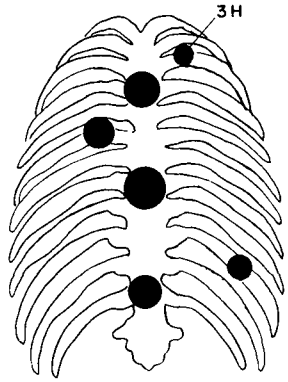

FIG. 7. CAP phantom, posterior aspect, shows size and position of lesions to be imaged.

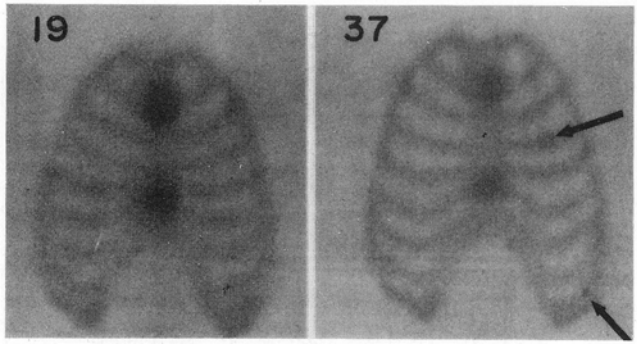

FIG. 8 CAP imaging phantom using high sensitivity collimator, anterior view. Note ability to visualize lesions indicated, 0.8 cm and 1.0 cm in diameter, 1.25 in. from collimator with 37 GP system, not seen with HP camera.

The Rollo phantom (Fig. 10) was used to calculate the "contrast efficiency function." This phantom was designed to simulate actual organ imaging by giving each lucite cell a specific object contrast ratio in relation to its activity void. These predetermined object contrast ratios are designed to simulate liver, heart, kidney, and thyroid imaging. The contrast efficiency function, Ec (r), is designed to quantitatively measure how well an imaging system will detect a spherical void of activity within an activity distribution (*3*). The function is calculated as follows:

$$\text{Ec (r)} = \frac{\text{Ci}}{\text{Co}}; \text{ where}$$

Co = object contrast of the phantom; and

Ci = image contrast, calculated as:

$$\frac{\text{(cell background} - \text{void activity)}}{\text{cell background}}$$

Theoretically, as camera resolution increases, Ec (r) approaches unity.

This function was evaluated for every camera using the

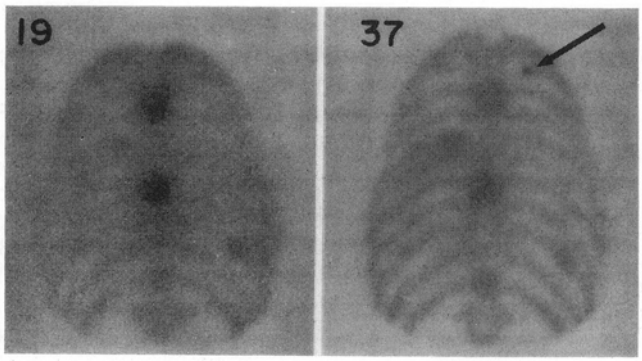

FIG. 9. CAP imaging phantom using high sensitivity collimator, posterior view. Note ability to visualize lesion indicated, 1.2 cm in diameter, 0.75 in. from collimator with 37 GP system, not seen with HP camera.

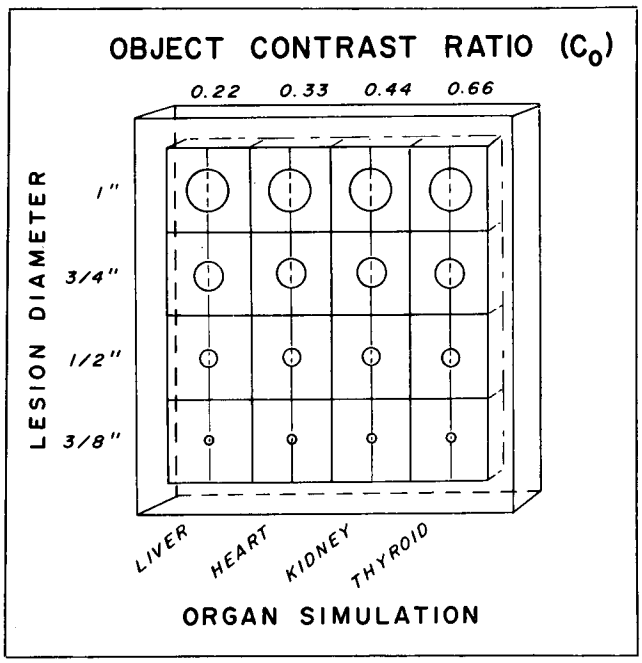

FIG. 10. Design of Rollo phantom used to calculate contrast efficiency function.

1 in. void of the simulated thyroid cell, having an object contrast (Co) of 0.66. Using the region-of-interest capability of every camera, identical area regions were established and counted over the void and the cell background. The 37PM-tube camera demonstrated an Ec (r) of 0.77 compared to an Ec (r) of 0.53 for the 19PM-tube camera.

Discussion

The 19PM-tube Pho/Gamma HP camera demonstrated a slight superiority in plane sensitivity—0.39 compared with 0.33 cpm/μCi/cm^2. These results are in agreement with a previous study (*4*), in which the plane sensitivity of the Pho/Gamma HP was compared to the Pho/Gamma IV, a camera similar to the 37 GP.

The Pho/Gamma 37 GP demonstrated a marked superiority in spatial resolution for every phantom studied. This is further verified by the calculated Ec (r), which was 0.77 for the 37PM-tube camera and 0.53 for the 19PM-tube camera. Since the PM tube type and specifications were unchanged, the increased number of PM tubes for the same area crystal seems to be primarily responsible for the increased spatial resolution. As demonstrated by the CAP organ phantoms, this increased resolution is directly related to the camera's ability to detect clinical pathology, especially in the range of 0.8- to 1.5-cm diameter lesions.

References

1. Hine G, Kirch D: Recent advances in gamma cameras. *Appl Radiology* 6: 194–200, 1977

2. Rollo FD: Evaluating Imaging Devices. In *Nuclear Medicine Physics, Instrumentation, and Agents,* FD Rollo, ed, St. Louis, C.V. Mosby, 1977, pp 436–452

3. Rollo FD: Technique for evaluating imaging devices. *Appl Radiology* 5: 195–198, 1976

4. Hine G, Paras P: Measurements of the performance parameters of gamma camera. Part I, HEW Publications(FDA)78–8049, 1977, p35